Controlling the Topological Sector of Magnetic Solitons in Exfoliated $Cr_{1/3}NbS_2$ Crystals

L. Wang,[1,2,*] N. Chepiga,[3] D.-K. Ki,[1] L. Li,[4] F. Li,[5] W. Zhu,[5] Y. Kato,[6] O. S. Ovchinnikova,[7] F. Mila,[3] I. Martin,[8] D. Mandrus,[4,9,10] and A. F. Morpurgo[1,†]

[1]*Department of Quantum Matter Physics and Group of Applied Physics, University of Geneva, 24 quai Ernest-Ansermet, CH-1211 Geneva, Switzerland*

[2]*Key Laboratory of Flexible Electronics (KLOFE) & Institute of Advanced Materials (IAM), Jiangsu National Synergetic Innovation Center for Advanced Materials (SICAM), Nanjing Tech University (NanjingTech), 30 South Puzhu Road, Nanjing 211816, China*

[3]*Institute of Physics, École Polytechnique Fédérale de Lausanne, 1015 Lausanne, Switzerland*

[4]*Department of Materials Science and Engineering, University of Tennessee, Knoxville, Tennessee 37996, USA*

[5]*Theoretical Division, T-4 and CNLS, Los Alamos National Laboratory, Los Alamos, New Mexico 87545, USA*

[6]*Department of Applied Physics, University of Tokyo, Hongo, 7-3-1, Bunkyo, Tokyo 113-8656, Japan*

[7]*Nanofabrication Research Laboraotry, Center for Nanophase Materials Sciences, Oak Ridge National Laboratory, Oak Ridge, Tennessee 37831-6493, USA*

[8]*Materials Science Division, Argonne National Laboratory, Argonne, Illinois 60439, USA*

[9]*Materials Science and Technology Division, Oak Ridge National Laboratory, Oak Ridge, Tennessee 37831, USA*

[10]*Department of Physics and Astronomy, University of Tennessee, Knoxville, Tennessee 37996, USA*

(Received 7 April 2017; published 23 June 2017)

We investigate manifestations of topological order in monoaxial helimagnet $Cr_{1/3}NbS_2$ by performing transport measurements on ultrathin crystals. Upon sweeping the magnetic field perpendicularly to the helical axis, crystals thicker than one helix pitch (48 nm) but much thinner than the magnetic domain size (~ 1 μm) are found to exhibit sharp and hysteretic resistance jumps. We show that these phenomena originate from transitions between topological sectors with a different number of magnetic solitons. This is confirmed by measurements on crystals thinner than 48 nm—in which the topological sector cannot change—that do not exhibit any jump or hysteresis. Our results show the ability to deterministically control the topological sector of finite-size $Cr_{1/3}NbS_2$ and to detect intersector transitions by transport measurements.

DOI: 10.1103/PhysRevLett.118.257203

The properties of many electronic systems are characterized by topological indices that allow all possible states to be grouped into distinct topological sectors [1–5]. Since topological indices assume discrete values, changes in the topological sector can only occur through abrupt transitions that can be detected experimentally. Investigating these transitions under controlled conditions and probing properties associated with "topological order," however, is not simple, as it requires the ability to tune the state of the system in a predefined topological sector, i.e., to deterministically set the topological indices of the system by acting on experimental parameters. Here we show that this level of control can be achieved by means of magnetoresistance measurements on mechanically exfoliated crystals of the monoaxial chiral helimagnet $Cr_{1/3}NbS_2$.

Our experiments build on earlier work that has established the key properties of $Cr_{1/3}NbS_2$, a layered material consisting of alternating NbS_2 and Cr planes [see Fig. 1(a)] [6–17]. At low temperature, the $S = 3/2$ spins on the Cr atoms order ferromagnetically in each plane, forming a helix that winds around the direction perpendicular to the planes [Fig. 1(b), the zero-field helix pitch L_0 is 48 nm] [9,11–14]. Lorentz microscopy has shown that the in-plane magnetic field B causes the helix to deform, resulting in a so-called chiral soliton lattice [12]. The lattice [Fig. 1(b)] consists of narrow regions in which the spins make a complete 2π revolution (the solitons), separated by stretches of ferromagnetically aligned spins, whose extension—which determines the lattice period L_B—increases upon increasing B [Fig. 1(c)] [12]. The observed microscopic evolution of the helix, as well as the detailed magnetic response of bulk crystals, conform quantitatively to a theoretical (one-dimensional) model proposed by Dzyaloshinskii over 50 years ago, comprising Heisenberg and Dzyaloshinskii-Moriya interactions between nearest neighboring spins (besides the Zeeman term in the presence of a magnetic field and a magnetic anisotropy term that forces the spins to point perpendicularly to the helix direction) [18,19].

Whenever it is spatially confined, the chiral soliton lattice in $Cr_{1/3}NbS_2$ is predicted to exhibit interesting phenomena [20–23]. Some of these phenomena have been observed recently in a small specimen (10 μm in linear dimensions) cut from bulk crystals, in which confinement originates from the presence of magnetic domains extending for approximately 1 μm in the helix direction [22]. Upon increasing B, the separation between solitons increases, so that their total number in each finite-size domain decreases. Since the number of solitons corresponds to the total spin winding number that is a topological index, the soliton number can only change through discrete transitions. These transitions

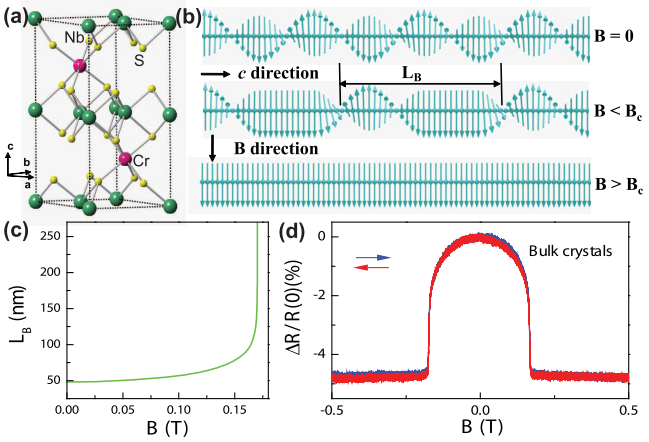

FIG. 1. (a) Structure of layered $Cr_{1/3}NbS_2$. The c-axis lattice constant is 1.21 nm. (b) Schematic illustration of the spin configurations along the c axis in bulk $Cr_{1/3}NbS_2$ (the arrows represent the magnetization in the Cr planes). Upon increasing magnetic field (B) in the ab plane, the $B = 0$ magnetic helix (top) is gradually transformed into a chiral soliton lattice with period L_B (middle), finally becoming ferromagnetic above the critical magnetic field (B_c; bottom). (c) In the process, the period L_B increases and diverges close to B_c (plot obtained from theoretical calculations based on the model discussed in the main text). (d) Magnetoresistance, $\Delta R/R(0) \equiv (R(B) - R(0))/R(0)$, of bulk $Cr_{1/3}NbS_2$ measured at 250 mK. The blue or red curve corresponds to measurements performed upon sweeping the in-plane field B in the direction indicated by the blue or red arrow. An abrupt resistance drop at $B_c \sim 0.17$ T with no hysteresis is observed.

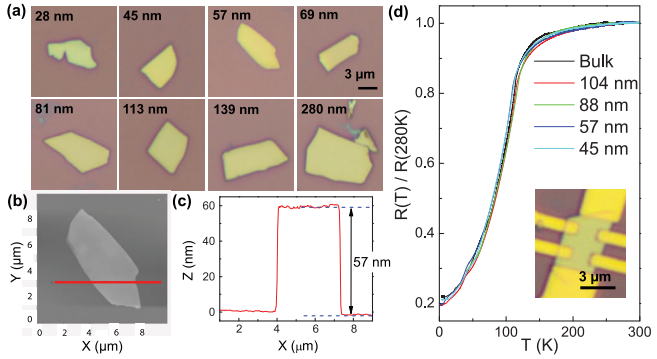

FIG. 2. (a) Optical microscope images of exfoliated $Cr_{1/3}NbS_2$ crystals with thicknesses between 28 nm and 280 nm. (b) Atomic force microscope image of the 57-nm-thick crystal, showing a flat and uniform surface, as visible in the thickness profile (c) taken along the red line. (d) Temperature dependence of the resistance $R(T)/R(280K)$ for crystals of different thicknesses (see legend). All curves merge together and exhibit a resistance drop starting around 130 K, the bulk transition temperature of the helimagnetic state. The inset in (d) shows an optical image of a device, with nanofabricated Ti/Au contacts. In all images, the scale bar is 3 μm.

have been detected by analyzing Lorentz microscope images [22]. It was argued that hysteresis and a sequence of jumps present in the magnetoresistance of small specimen, but absent in bulk crystals [see Fig. 1(d)], are a transport manifestation of the changes in soliton number [22,23]. This conclusion is very interesting, as it implies the ability to probe topological aspects of the magnetic state of $Cr_{1/3}NbS_2$ by monitoring transport properties. Its validity is, however, unclear because the magnetoresistance jumps could not be directly linked to specific changes in the soliton configuration, and because it was not ruled out that the jumps may originate from domain switching.

To avoid these problems, we investigate these same phenomena by working with $Cr_{1/3}NbS_2$ crystals much thinner than the magnetic domain size. Figure 2(a) shows optical microscope images of a selection of crystals having thickness (t) between 28 and 300 nm, whose surfaces are parallel to the NbS_2 and the Cr planes. The magnetic helix is oriented perpendicular to the substrate, so that the crystal thickness determines the number of solitons present at $B = 0$. We produced these crystals, up to 500 times thinner than the specimen studied in Ref. [22], by means of mechanical exfoliation, following the same procedure used to extract graphene from graphite. Exfoliation is more difficult for $Cr_{1/3}NbS_2$ because of strong chemical bonds between the Cr and S atoms; nevertheless, atomic force microscope images [see Figs. 2(b) and 2(c)] show that the crystal surface is flat and uniform.

Transport through $Cr_{1/3}NbS_2$ crystals as thin as the ones discussed here had not been investigated earlier and it is important to identify which properties depend on thickness and which do not. Figure 2(d) shows that all exfoliated crystals exhibit the same temperature dependence of the resistance (identical to that of the bulk). A pronounced decrease in resistance starts around $T = 130$ K, corresponding to the transition temperature T_c to the helimagnetic state. Since T_c is determined by the strength of the microscopic interactions between nearest neighboring spins (and—in the range investigated here—not by the thickness) this behavior is not surprising [24]. Nevertheless, the excellent reproducibility upon varying the thickness is worth commenting on, as it indicates the absence of any significant material degradation (not warranted *a priori* for thin crystals exposed to air during exfoliation and device fabrication).

The relative change in resistance upon the application of an in-plane magnetic field, $\Delta R/R(0) \equiv (R(B) - R(0))/R(0)$, is shown in Figs. 3(a)–3(d) for several crystals containing one [(a),(b); $t = 57$ nm and 79 nm, respectively], two [(c); $t = 113$ nm], and five [(d); $t = 280$ nm] complete helix periods at $B = 0$. The behavior is representative of what we observed in more than 10 devices realized with crystal having a thickness between approximately 50 and 300 nm, exhibiting common features and systematic trends. For these crystals, hysteresis in the magnetoresistance upon reversing the sweeping direction of the applied field is always present, and is accompanied by sharp jumps. The phenomena cannot originate from

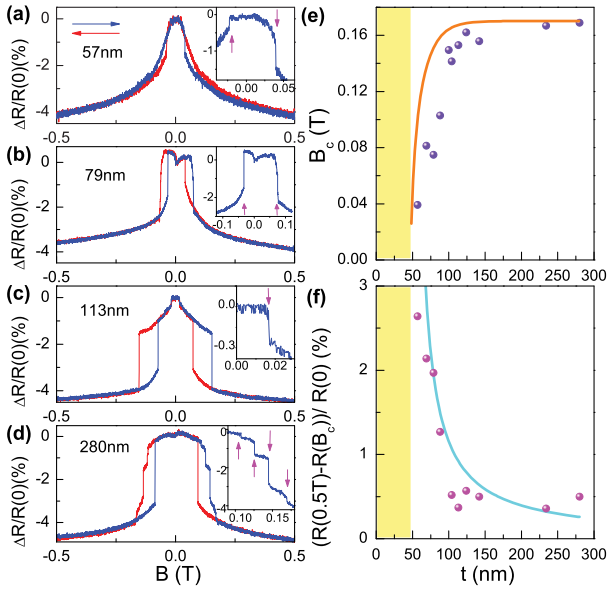

FIG. 3. (a)–(d) Evolution of the magnetoresistance, $\Delta R/R(0)$, measured at 250 mK on $Cr_{1/3}NbS_2$ crystals of different thickness (see legends; blue or red curve represents data taken while sweeping B in the direction indicated by the arrows). Resistance jumps and pronounced hysteresis are seen, absent in bulk $Cr_{1/3}NbS_2$ [see Fig. 1(d)]. The insets zoom-in on a small B range to make the smaller jumps visible. (e) Thickness dependence of the critical field B_c, corresponding to the highest value of B at which a resistance jump is observed. The experimental data (dots) are in good agreement with calculations (solid line). The resistance continues to decrease for $B > B_c$, as shown in (f) by plotting $(R(0.5T) - R(B_c))/R(0)$ versus t. The data (dots) approximately exhibit a $1/(t - L_0)$ dependence (solid line) expected as the phenomenon originates from the alignment of spins close to the crystal surfaces. The yellow regions in (e) and (f) denote the thickness range below L_0.

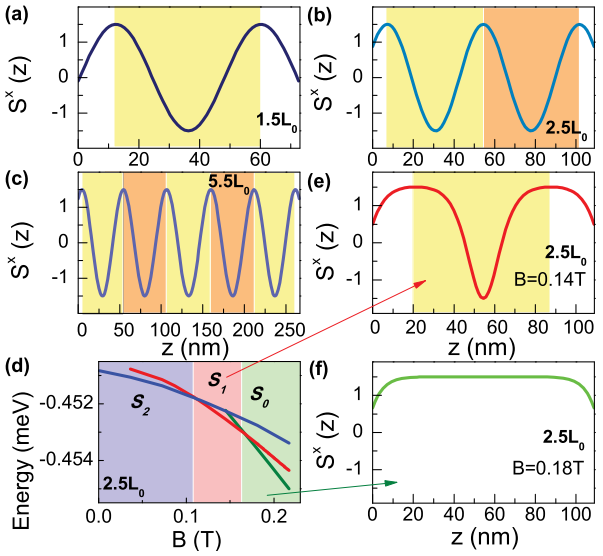

FIG. 4. (a)–(c) Lowest-energy configuration of the spin helix at $B = 0$, represented by the x component of spins on the Cr atoms (S^x), calculated using the model discussed in the main text for crystals with $t = 1.5\ L_0$, $2.5\ L_0$, and $5.5\ L_0$ ($L_0 = 48$ nm). The colored areas mark complete spin windings, corresponding to the presence of one (a), two (b), and five (c) magnetic solitons. (d) The blue, red, and green lines correspond to the lowest energy of configurations containing two, one, and zero solitons, calculated as a function of B for a crystal with $t = 2.5\ L_0$. At low B (blue shaded region) configurations containing two solitons [panel (b)] have the lowest energy; for intermediate values of B (red shaded region) configurations with one soliton [panel (e)] have the lowest energy; for the higher field, configurations with no solitons [panel (f)] are energetically favorable.

magnetic domains, since all crystals are significantly thinner than the domain size [22]. We find that the number of jumps tends to increase with increasing the crystal thickness, seemingly correlating with the number of complete periods present in the magnetic helix at $B = 0$ (determined by t/L_0 where L_0 is the helix pitch). For instance, the crystals in Figs. 3(a) and 3(b) contain one full period and exhibit one jump, the crystal with $t = 113$ nm [Fig. 3(c)] contains two full periods and exhibits two jumps. The $t = 280$ nm crystal contains five full periods at $B = 0$, and four jumps are observed, but the jump at $B \sim 0.17$ T appears to be smeared, suggesting that it may originate from two jumps that are not resolved individually. The magnetic field at which the last jump occurs systematically increases with increasing crystal thickness, as shown in Fig. 3(e). Finally, the total change in the relative magnetoresistance measured after the last jump decreases with increasing thickness [see Fig. 3(f); this same quantity vanishes in bulk crystals].

All the observed trends can be understood in terms of a theoretical model known to properly describe the magnetic state of $Cr_{1/3}NbS_2$ (the model is discussed in several papers and here we only recall the key conceptual aspects; see also the Supplemental Material [25]) [12,14–16,21,26,27]. The model enables the spin configuration to be determined through the minimization of the system energy expressed as a functional of the local magnetization. Its validity for $Cr_{1/3}NbS_2$ has been established by direct comparison with Lorentz microscopy experiments and magnetization measurements, which enable the model parameters to be extracted quantitatively [12,22]. The model has also been applied to strained MnSi thin films [28,29] [30] to interpret magnetotransport data closely related to the ones discussed here. In this context, it was assumed that all changes causing a better aligned spin configuration result in smaller measured resistance [25].

In this same spirit, we reproduce some of the known results by solving the model numerically as a function of B for crystals of different thicknesses, and we use the numerical solutions to illustrate the aspects of the behavior that account for the experimentally observed trends [25]. Figures 4(a)–4(c) show the lowest energy spin configuration—represented by the x component of the spin on the chromium atoms planes—calculated at $B = 0$ for crystals having $t = 1.5\ L_0$, $2.5\ L_0$, $5.5\ L_0$

(hosting, respectively, 1, 2, and 5 complete spin windings). For any given thickness, we calculate the spin configuration that minimizes the energy as the magnetic field is increased. This is done by minimizing the energy in each topological sector separately and comparing the resulting values to determine the absolute minimum. The outcome of this procedure is illustrated in Fig. 4(d) for the $t = 2.5\ L_0$ crystal. The lowest energy state at $B = 0$ contains two magnetic solitons [Fig. 4(b)], but at a sufficiently large in-plane magnetic field the state with one soliton [Fig. 4(e)] becomes energetically favorable. At even larger B, the state with no solitons has the lowest energy, and all the spins are aligned, except those in proximity of the surfaces [Fig. 4(f)]. Past this field, any further increase in B only causes a gradual alignment of these spins. Such a sequence of transitions, with the number of solitons decreasing monotonically upon increasing B, is what the model predicts for all values of t (not only for $t = 2.5\ L_0$).

This behavior accounts for all the experimentally observed trends. At each transition the resistance decreases, exhibiting a jump, because in configurations with a smaller number of solitons the spins are on average better aligned with the applied field [25]. Therefore, the total number of jumps in the magnetoresistance equals the number of transitions between states with a different number of solitons, which can be calculated (and typically corresponds to the largest integer smaller than t/L_0). This is indeed in line with the experimental observations. Hysteresis is expected theoretically because configurations with the number of solitons differing by one have different parity relative to the center of the crystals, so that whenever the system undergoes a transition, the spin configuration changes abruptly over the entire crystal. As a result, there is an energy barrier between solutions with a different number of solitons, so that upon small variation of B the system stays in the local minimum even when this is not the lowest energy configuration. The values of B at which the transitions occur can be calculated as a function of t and compared to the experiments. We focus on the last transition observed upon increasing B past B_c (i.e., the transition between the configurations containing 1 and 0 solitons), because this transition is present in all crystals with $t > 50$ nm, giving us enough statistics for a meaningful quantitative comparison [31]. The data are systematic and the agreement with calculation is very good [see Fig. 3(e)]. Finally, the model also explains the trend seen in the magnitude of the magnetoresistance measured upon varying B past B_c. In this regime the magnetoresistance decreases because the spins next to the two crystals' surfaces [see Fig. 4(f)] align progressively to the applied field as B is increased. The gradual decrease in resistance is therefore a surface effect whose magnitude should be expected to decay approximately as $1/(t - L_0)$ and vanish in the bulk. This indeed agrees with the experiments [see Fig. 3(f), and Fig. 1(d) for the behavior of the bulk].

The relevance of these results stems from the fact that, contrary to all earlier work on $Cr_{1/3}NbS_2$ [22,23], the crystals investigated here are substantially thinner than the magnetic

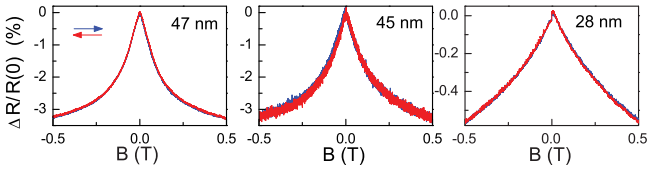

FIG. 5. Magnetoresistance $\Delta R/R(0)$ of crystals thinner than the helix pitch ($L_0 = 48$ nm) measured at 250 mK. The blue or red curves represent data measured while sweeping B in opposite directions, as indicated by the arrows. In all cases, only a continuous decrease of the resistance is observed, and no jumps or hysteresis is present.

domain size, so that domain switching can be excluded as a possible origin of the phenomena. This and the agreement between observations and theoretically expected trends allow us to conclude that the observed jumps and the hysteresis do originate from transitions between states with a different soliton number. The use of exfoliated crystals enables us to obtain further evidence supporting this conclusion, as it allows us to investigate crystals thinner than the helix pitch, a regime that has not been explored so far. No jumps and hysteresis in the magnetoresistance should be expected, because in this regime the soliton number vanishes for all values of B, and no topological transition can occur. Figure 5 shows that this is indeed the case: in all $Cr_{1/3}NbS_2$ crystals thinner than the helix pitch at $B = 0$ only a negative magnetoresistance is observed due to the gradual spin alignment upon increasing B. No jumps or hysteresis are present. This drastic qualitative difference in behavior observed upon changing the crystal thickness by only a few nanometers is striking. It provides conclusive evidence that in $Cr_{1/3}NbS_2$ the topological sector of the system can be controlled and probed by transport measurements.

In summary, we have performed experiments on very thin exfoliated crystals showing that the number of solitons in $Cr_{1/3}NbS_2$ can be controlled by selecting the appropriate crystal thickness and by acting on the applied field. The experiments further show that changes in the number of solitons manifest themselves in hysteretic magnetoresistance jumps. These results imply that the topological sector of the system can be deterministically controlled and probed by transport measurements.

L. W., D.-K. K., and A. F. M. are indebted to A. Ferreira for continuous technical assistance. N. C., F. M., and A. F. M. acknowledge financial support from the Swiss National Science Foundation. A. F. M. gratefully acknowledges financial support from the EU Graphene Flagship project. L. L. and D. M. acknowledge support from the National Science Foundation under Grant No. DMR-1410428. F. L. and W. Z. are supported by LANL through LDRD program. I. M. acknowledges support from Department of Energy, Office of Basic Energy Science, Materials Science and Engineering Division. O. S. O. is supported by the Laboratory Directed Research and Development Program of Oak Ridge National Laboratory, managed by UT-Battelle, LLC, for the U. S. Department of Energy.

*Corresponding author.
iamlwang@njtech.edu.cn
†Corresponding author.
Alberto.Morpurgo@unige.ch

[1] M. I. Monastyrskiĭ, *Topology of Gauge Fields and Condensed Matter* (Plenum Press, New York, 1993).
[2] G. E. Volovik, *The Universe in a Helium Droplet*, International Series of Monographs on Physics (Clarendon Press, Oxford; Oxford University Press, New York, 2003).
[3] A. Altland and B. Simons, *Condensed Matter Field Theory*, 2nd ed. (Cambridge University Press, Cambridge, England and New York, 2010).
[4] E. Fradkin, *Field Theories of Condensed Matter Physics*, 2nd ed. (Cambridge University Press, Cambridge, England, 2013).
[5] X.-L. Qi and S.-C. Zhang, Rev. Mod. Phys. **83**, 1057 (2011).
[6] S. S. P. Parkin and R. H. Friend, Philos. Mag. B **41**, 65 (1980).
[7] S. S. P. Parkin and R. H. Friend, Physica (Amsterdam) **99**, 219 (1980).
[8] T. Moriya and T. Miyadai, Solid State Commun. **42**, 209 (1982).
[9] T. Miyadai, K. Kikuchi, H. Kondo, S. Sakka, M. Arai, and Y. Ishikawa, J. Phys. Soc. Jpn. **52**, 1394 (1983).
[10] Y. A. Izyumov, Sov. Phys. Usp. **27**, 845 (1984).
[11] Y. Kousaka, Y. Nakao, J. Kishine, M. Akita, K. Inoue, and J. Akimitsu, Nucl. Instrum. Methods Phys. Res., Sect. A **600**, 250 (2009).
[12] Y. Togawa, T. Koyama, K. Takayanagi, S. Mori, Y. Kousaka, J. Akimitsu, S. Nishihara, K. Inoue, A. S. Ovchinnikov, and J. Kishine, Phys. Rev. Lett. **108**, 107202 (2012).
[13] N. J. Ghimire, M. A. McGuire, D. S. Parker, B. Sipos, S. Tang, J. Q. Yan, B. C. Sales, and D. Mandrus, Phys. Rev. B **87**, 104403 (2013).
[14] Y. Togawa, Y. Kousaka, S. Nishihara, K. Inoue, J. Akimitsu, A. S. Ovchinnikov, and J. Kishine, Phys. Rev. Lett. **111**, 197204 (2013).
[15] B. J. Chapman, A. C. Bornstein, N. J. Ghimire, D. Mandrus, and M. Lee, Appl. Phys. Lett. **105**, 072405 (2014).
[16] A. C. Bornstein, B. J. Chapman, N. J. Ghimire, D. G. Mandrus, D. S. Parker, and M. Lee, Phys. Rev. B **91**, 184401 (2015).
[17] K. Tsuruta, M. Mito, H. Deguchi, J. Kishine, Y. Kousaka, J. Akimitsu, and K. Inoue, Phys. Rev. B **93**, 104402 (2016).
[18] I. E. Dzyaloshinskii, J. Phys. Chem. Solids **4**, 241 (1958).
[19] T. Moriya, Phys. Rev. **120**, 91 (1960).
[20] J. I. Kishine, I. G. Bostrem, A. S. Ovchinnikov, and V. E. Sinitsyn, Phys. Rev. B **89**, 014419 (2014).
[21] K. Tsuruta, M. Mito, Y. Kousaka, J. Akimitsu, J. Kishine, Y. Togawa, H. Ohsumi, and K. Inoue, J. Phys. Soc. Jpn. **85**, 013707 (2016).
[22] Y. Togawa, T. Koyama, Y. Nishimori, Y. Matsumoto, S. McVitie, D. McGrouther, R. L. Stamps, Y. Kousaka, J. Akimitsu, S. Nishihara, K. Inoue, I. G. Bostrem, V. E. Sinitsyn, A. S. Ovchinnikov, and J. Kishine, Phys. Rev. B **92**, 220412 (2015).
[23] K. Tsuruta, M. Mito, Y. Kousaka, J. Akimitsu, J. Kishine, Y. Togawa, and K. Inoue, J. Appl. Phys. **120**, 143901 (2016).
[24] P. Bak and M. H. Jensen, J. Phys. C **13**, L881 (1980).
[25] See Supplemental Material at http://link.aps.org/supplemental/10.1103/PhysRevLett.118.257203 for a detailed description of our model, the values of parameters used for the numerical calculations, and the results.
[26] A. B. Borisov, J. I. Kishine, I. G. Bostrem, and A. S. Ovchinnikov, Phys. Rev. B **79**, 134436 (2009).
[27] J. I. Kishine, I. V. Proskurin, and A. S. Ovchinnikov, Phys. Rev. Lett. **107**, 017205 (2011).
[28] M. N. Wilson, E. A. Karhu, D. P. Lake, A. S. Quigley, S. Meynell, A. N. Bogdanov, H. Fritzsche, U. K. Rößler, and T. L. Monchesky, Phys. Rev. B **88**, 214420 (2013).
[29] E. A. Karhu, U. K. Rößler, A. N. Bogdanov, S. Kahwaji, B. J. Kirby, H. Fritzsche, M. D. Robertson, C. F. Majkrzak, and T. L. Monchesky, Phys. Rev. B **85**, 094429 (2012).
[30] Bulk MnSi is not a chiral helical magnet, but MnSi thin films are in a narrow range of thicknesses, due to strain from the substrate [28,29].
[31] The B values at which the transitions occur depend on thickness that—for exfoliated crystals—cannot be deterministically controlled. This makes it difficult to compare the precise value of magnetic field for which a generic resistance jump is expected to occur with theory. Since devices of all thicknesses $t > L_0$ exhibit the jump corresponding to the transition to the ferromagnetic state, for this transition it is nevertheless possible to obtain enough data to make a statistically significant comparison.